# Multi-omics integration reveals sex-based differences in the circulating extracellular vesicle lipidome and miRNome of alcohol use disorder patients

Carla Perpiñá-Clérigues[1,2], Susana Mellado[1], Cristina Galiana-Roselló[2], Saritha Kodikara[3], Blanca Martín-Urdiales[1], Miguel Marcos[4], Kim-Anh Lê Cao[3], Francisco García-García[2]*, and María Pascual[1]*

[1]Department of Physiology, School of Medicine and Dentistry, University of Valencia, 46010 Valencia, Spain

[2]Computational Biomedicine Laboratory, Príncipe Felipe Research Center, 46012 Valencia, Spain

[3]Melbourne Integrative Genomics, School of Mathematics and Statistics, University of Melbourne, Melbourne, VIC, Australia

[4]Department of Internal Medicine, University Hospital of Salamanca, University of Salamanca, Institute of Biomedical Research of Salamanca (IBSAL), 37007 Salamanca, Spain

* These authors contributed equally to this work

Corresponding authors:

María Pascual, Department of Physiology, University of Valencia, Avda. Blasco Ibáñez, 15. 46010 Valencia, Spain. Tel: (+34) 961625635, Fax: (+34) 963864642. E-mail: maria.pascual@uv.es

Francisco García-García, Computational Biomedicine Laboratory, Príncipe Felipe Research Center, C/ Eduardo Primo Yúfera, 3. 46012 Valencia, Spain. Tel: (+34) 963289680, Fax: (+34) 963289701. E-mail: fgarcia@cipf.es

**Keywords:** lipidomics, miRNA transcriptomics, multi-omics, extracellular vesicles, alcohol use disorder, sex-based differences.

**Running title:** Multi-omics of EVs reveals sex effects in AUD

## Abstract

### Background

Integrated multi-omics and extracellular vesicle (EV) analysis are emerging as powerful, complementary strategies for biomarker discovery. These approaches offer promising tools to enhance early detection, diagnosis, and treatment of alcohol use disorder (AUD), a prevalent and globally significant neuropsychiatric condition.

### Methodology

Here we applied an integrated miRNomic and lipidomic approach to analyze plasma EVs from AUD patients and controls of both sexes to gain a comprehensive understanding of the underlying molecular mechanisms.

### Results

We identified an AUD signature with predictive potential for diagnostic and prognostic applications. Individual features (e.g., hsa-miR-99b-3p, hsa-miR-556-5p, Cer_NDS d39:1, and PI 18:0_18:2) represented important components; however, the strength of this signature lay in the combined profile rather than isolated markers. We also revealed an AUD-sex signature that provided insight into how biological responses to alcohol differ between females and males (including features such as hsa-miR-1301-3p and PC 39:4), which also underscored the power of multi-omic integration. The individual miRNome approach also revealed an opposite functional alteration by sex in various alcohol related systems, such as pathways associated with immunity, oxidative stress, and autophagy.

### Conclusions

While addressing the long-standing underrepresentation of females in alcohol-related research, this collective work also represents the first study to integrate EV-derived miRNA and lipid data to uncover sex-related pathophysiological pathways in AUD. Together, our findings underscore the added value of multi-omics integration in identifying clinically relevant molecular signatures of disease; this sex-informed approach offers a promising path toward more personalized diagnostic tools and therapeutic strategies in AUD.

## Introduction

Multi-omics has emerged as a result of advances in various omic-based technologies (including genomics and metabolomics) alongside enhanced computing capabilities, which have enabled an improved understanding of the complex molecular interplay between health and disease by combining the power of individual data types (1). This analytical approach measures different layers of cellular information, facilitating the identification of molecular signatures and biomarkers for mechanism-based classifications and tailored therapeutic interventions (2,3) and offering deep insight into the pathophysiology of disease states (4). The use of multivariate approaches - facilitated by this novel integrative analysis - has enabled the expansion of results obtained through univariate methods (5) to predict, prevent, and treat disease more precisely by considering each individual's genetics, environment, and lifestyle factors (1).

Recent reports support the applicability of transcriptomics and lipidomics in biomarker identification and pathology elucidation. Transcriptomics, including miRNA analysis, represents a robust methodology for determining mRNA/miRNA expression via high-throughput RNA-sequencing (RNA-seq) (4). Although lipidomics represents an effective approach to analyzing changes to the levels of endogenous lipids in biological systems (4), alterations in lipid levels/enzymatic reactions may not accurately identify pathways altered in specific pathologies. We can address this gap by integrating various omic-based technologies, which offer a more comprehensive view of alterations in complex biological processes induced by any pathological condition. A combined miRNomic and lipidomic approach has the potential to generate extensive datasets that will support the identification of associations between miRNAs and lipids/enzymes and uncover molecular mechanisms based on high-throughput data.

An increasing number of studies into alcohol consumption have applied transcriptomic and lipidomic technologies to understand the molecular mechanisms underlying alcohol use disorders (AUDs) and search for possible disease biomarkers (6–8). Alcohol remains a widely misused substance, with the World Health Organization reporting that abuse causes approximately 2.6 million deaths per year (9). Early AUD identification and treatment potentially reduce the risk of developing

related pathologies (e.g., certain types of cancer, diseases associated with reduced immunity, and increased infections, infertility, and depression) (10). Overall, the lack of specific and sensitive biomarkers for AUD diagnosis and effective treatment approaches has prompted the need for the application of novel technologies such as integrated multi-omics. Multi-omics enables the simultaneous analysis of miRNAs and lipids, for example, to provide insights into miRNomic and lipidomic alterations following alcohol consumption, which will help to map complex relationships.

Extracellular vesicles (EVs), which carry miRNAs and lipids, act as critical intercellular mediators, particularly under cellular stress or damage. Unlike synthetic drug delivery systems, EVs demonstrate superior biocompatibility, extended biodistribution, and low immunogenicity (11). These properties position EVs and their content as valuable non-invasive biomarkers and therapeutic targets for diverse pathologies, including neurodegenerative disorders (12–14). We previously identified AUD-related lipidomic fingerprints in plasma EVs from AUD females and males (6); here, the first implementation of an integrated multi-omics approach (combining transcriptomics and lipidomics) using plasma EVs isolated from AUD males and females has enabled a more comprehensive understanding of the biological processes involved following excessive alcohol consumption. Our results reveal an AUD signature for predictive modeling, which could contribute to prognostic and diagnostic applications, and an AUD-Sex signature, which captures sex-specific molecular biomarkers, thereby enabling a deeper understanding of how biological responses to alcohol differ between females and males.

## Materials and Methods

### Human Subjects and Experimental Design

This study includes AUD patients (according to DSM-5 criteria) referred to the Alcoholism Unit of the University Hospital of Salamanca (Spain) (15). Healthy volunteers who reported drinking <□15 g of ethanol/day were also recruited as control patients. AUD patients and healthy volunteers were previously recruited and described in Perpiñá-Clerigués *et al*. 2024 (6). All individuals gave their informed consent to participate, and the study was approved by the Ethics Committee of the

University Hospital of Salamanca (Spain). Plasma samples were snap-frozen in liquid nitrogen and stored at -80 °C until further use. At this point, samples were processed for EV isolation.

Investigating the effects of alcohol consumption on miRNA and lipid content in EVs and exploring the molecular basis underlying sex-specific responses used the strategy depicted in Figure 1. Lipids and miRNAs were obtained from plasma EVs of AUD and control patients. The lipidome and miRNome were analyzed independently before the data were integrated to examine reciprocal regulation. The lipidome analysis was previously conducted by Perpiñá-Clérigues et al. (6), who detailed the workflow from lipid extraction to bioinformatics characterization of EV lipid content across experimental groups. The miRNome analysis involved four key steps: (i) extraction and sequencing of EV miRNAs; (ii) preprocessing, mapping, and normalization; (iii) differential expression analysis; and (iv) functional profiling. The integration of miRNomic and lipidomic datasets begins with the normalization of expression matrices. Table S1 details the samples employed. All bioinformatics and statistical analyses were performed using R software v.4.3.2 (16).

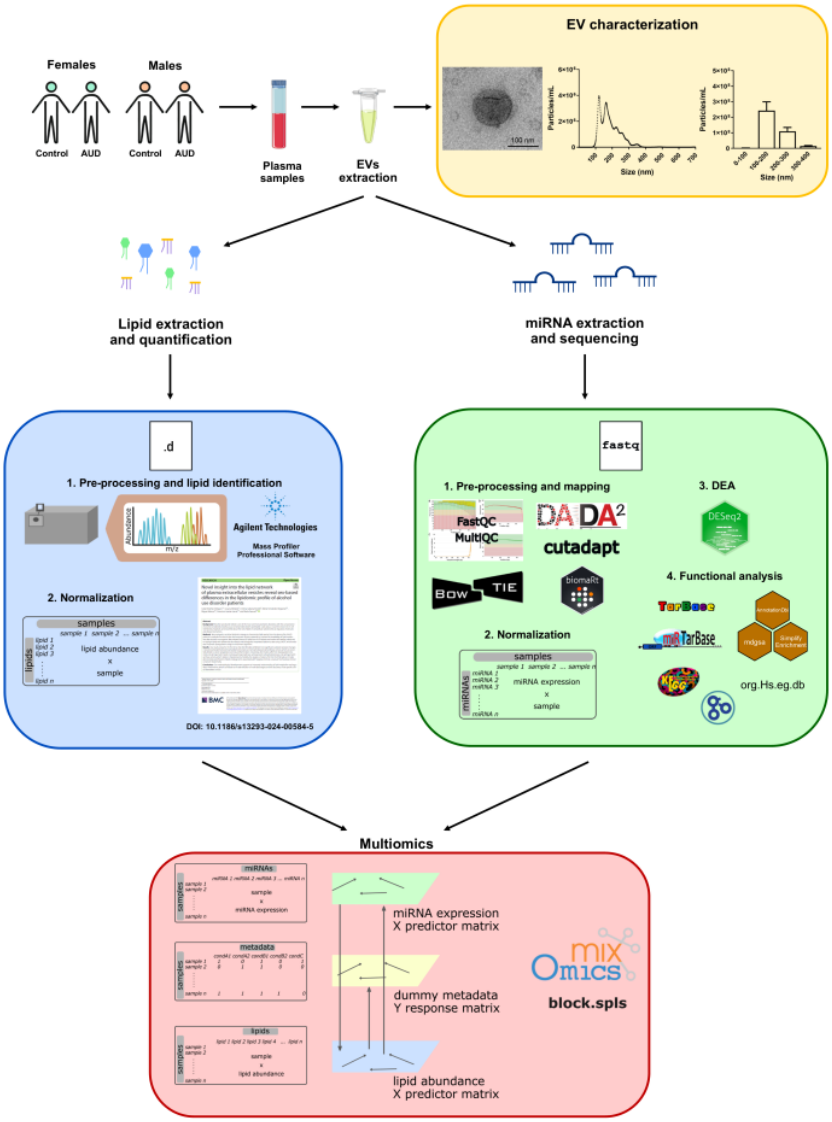


**Figure 1. Experimental design and workflow.** Lipids and miRNAs were extracted from plasma extracellular vesicles (EVs) of alcohol use disorder (AUD) patients and healthy individuals of both sexes. After data normalization for lipidomics and transcriptomics, miRNA data underwent differential expression analysis (DEA) and functional profiling. The implementation of the mixOmics R package applied the block sparse partial least squares (sPLS) method for multi-omics integration.

## EV Isolation and Characterization

Human plasma EVs were isolated using a total exosome isolation kit (4484450; Invitrogen, USA) following the manufacturer's instructions. 250 µL of initial plasma was employed to isolate EVs, which were collected and frozen at -80 °C until processing. Freshly isolated EVs were resuspended in PBS for characterization by transmission electron microscopy (TEM) and nanoparticle

tracking analysis (NTA) (Figure 1), as previously described by Ibáñez et al. (17). For TEM, EV preparations were examined under a FEI Tecnai G2 Spirit TEM (FEI Europe, Eindhoven, The Netherlands) with a Morada digital camera (Olympus Soft Image Solutions GmbH, Münster, Germany). The absolute size range and concentration of EVs were analyzed by NTA using a NanoSight NS300 Malvern (NanoSight Ltd., Minton Park, UK).

**RNA Extraction and Sequencing**

Total RNA from plasma EVs was isolated using the Total Exosome RNA Isolation Kit (Invitrogen, Waltham, MA, USA), following the manufacturer's instructions. The construction of miRNA libraries was performed using the TruSeq Small RNA Library Preparation Kit from Illumina (San Diego, CA, USA) at the Genomics and Genetics Service of the Príncipe Felipe Research Center (Valencia, Spain). RNA transcripts were first converted into complementary (c)DNA libraries, followed by quality and quantity assessments employing High Sensitivity D1000 ScreenTape for TapeStation System (Agilent Technologies, Santa Clara, CA, USA). The final libraries were pooled in equimolar concentration for sequencing in the MiSeq™ System (Illumina) through MiSeq™ Reagent Nano Kit v2 (Illumina) with 1 x 50 bp read length. Next-generation sequencing was performed at the Centre for Genomic Regulation (CRG) in Barcelona (Spain). The raw data generated by the high-throughput sequencing of miRNA were exported as fastq files.

To validate the miRNA levels from plasma EVs, the total miRNA was reverse transcribed using the TaqMan™ Advanced miRNA Assays (Thermo Fisher Scientific, Waltham, MA, USA). Real-time quantitative PCR (RT-qPCR) was performed using a QuantStudio™ 5 Real-Time PCR System (Applied Biosystems, Waltham, MA, USA). miRNAs were amplified using the TaqMan™ Fast Advanced Master Mix (Thermo Fisher Scientific), with the *U6* small nucleolar RNA used as an internal control. All RT-qPCR runs included non-template controls. Experiments were performed in triplicate. The quantification of expression (fold change) from the Cq data was calculated by the ΔΔCq method (Schmittgen and Livak, 2008) by the QuantStudio™ Design & Analysis Software (Applied Biosystems). Details of the nucleotide sequences of the used miRNA assays can be found in the Supplementary Material (Table S2).

**Processing and Mapping**

Raw sequencing reads underwent preprocessing using DADA2 (v.1.30.0) (18) and Cutadapt (v.4.6) (19). Reads were filtered based on a length threshold of 17–35 nucleotides and a Phred quality score of 30, ensuring high-quality sequences. The Illumina adapter sequences were removed before downstream analysis. After adapter removal, the trimmed sequences were aligned using Bowtie2 (v.2.5.3) (20) against a curated reference database of mature miRNA sequences from *Homo sapiens* as provided by miRBase (mature.fa) (21). The alignment parameters (-L 6 -i S,0,0.5 --ignore-quals --norc --score-min L,-1,-0.6 -D 20 --very-sensitive) were adapted from Locati et al. (22), optimizing sensitivity and specificity for small RNA alignment. Read counts were extracted directly from the resulting SAM files. Unique and multi-mapped reads were separated using Bash grep, with only uniquely mapped reads retained for quantification. This approach minimizes biases associated with ambiguous mapping while preserving the integrity of miRNA expression profiles.

**Exploratory Analysis and Normalization of miRNA Profiles**

Custom R scripts utilizing the DESeq2 package (v.1.42.1) (23) were used for both filtering and normalization. miRNAs were filtered to retain those with at least 10 reads in three or more samples. Subsequently, the median ratio normalization method implemented in DESeq2 was applied to adjust for differences in sequencing depth and RNA composition. Evaluating sample distribution across experimental groups and identifying potential anomalies or batch effects employed an exploratory analysis using boxplots, principal component analysis (PCA), and clustering techniques. These analyses were conducted before and after normalization to detect systematic biases and ensure data quality for downstream analyses.

**Differential Expression Analysis of miRNAs**

Identifying differentially expressed miRNAs employed DESeq2 (23). P-values were adjusted for multiple testing using the Benjamini–Hochberg (BH) method (24), with statistically significant miRNAs defined as those with a BH-adjusted p-value $\leq 0.05$.

Three primary comparisons were performed to assess sex-specific effects of AUD:

1. AUD Impact in Females (**IF**) assesses the differences between AUD females and control females (AUD.Females - Control.Females)
2. AUD Impact in Males (**IM**) assesses the differences between AUD males and control males (AUD.Males - Control.Males)
3. Impact of Sex in AUD (**IS**) assesses the differences between IF and IM (AUD.Females - Control.Females) - (AUD.Males - Control.Males)

The IF and IM comparisons identified miRNAs altered in AUD within each sex, while the IS comparison revealed miRNAs whose response to AUD differed significantly between sexes, accounting for baseline sex differences observed in healthy individuals.

Expression changes were quantified using log fold change (LFC), where the absolute value represents the magnitude of change and the sign indicates direction. A positive LFC indicates higher expression in the first group (AUD groups for IF/IM; females for IS), while a negative LFC indicates higher expression in the second group (controls for IF/IM; males for IS). For the IS comparison, which examines sex-dependent responses to AUD, the interpretation requires careful consideration. To resolve these scenarios, individual miRNA trends in IF and IM must be cross-referenced (Figure S1, "*Help*" section of our website [https://carpercle.shinyapps.io/SexEVEthOmics/]).

A complementary analysis examined combined AUD versus control samples (without sex stratification) to assess whether sex-specific analysis provided additional insights (*Supplementary Material*).

**Functional Profiling of miRNAs**

Investigating the functional implications of altered miRNA expression first linked differentially expressed miRNAs to their experimentally validated target genes using combined data from TarBase (25) and miRTarBase (26). Next, the differential expression levels of miRNAs were transferred to their target genes using the mdgsa package (v.0.99.2) (27), which considers statistical significance (p-value) and the direction of regulation (LFC sign). This set of target genes, sorted by the transfer of differential expression levels of their regulatory miRNAs, was then functionally characterized, providing a comprehensive miRNA regulatory model that reflects the cumulative effect

of multiple miRNAs on a given target. Functional enrichment analysis examined Gene Ontology (GO) annotations (28) and Kyoto Encyclopedia of Genes and Genomes (KEGG) pathways (29). Annotations were retrieved using the org.Hs.eg.db R package (v. 3.18.0) (30), which maps gene identifiers to their directly associated GO and KEGG terms. P-values were adjusted for multiple testing using the BH method (24), and terms/pathways with a BH-adjusted p-value $\leq 0.05$ were considered statistically significant. The absolute value and sign of log odds ratios (LORs) indicate the magnitude of change and the direction to detect pathway enrichment activity. Significant terms (BH-adjusted $p \leq 0.05$) with opposing LORs between sexes (indicating divergent regulatory impacts) were prioritized. Visualization and results representation were performed using simplifyEnrichment (31), which organizes terms based on semantic similarity (threshold = 0.8). Additionally, dot plots were generated for specific terms and pathways to enhance the interpretation of the miRNA regulatory network in the context of disease pathology.

**Multi-omic Integration**

Data were analyzed using processed and normalized results from previous univariate analyses, considering the distinct characteristics of each dataset. Prior to applying the integration approach, an sPLS analysis of the miRNA-lipid datasets was conducted to determine whether the information from both datasets agreed and reflected the AUD-sex condition. Then, a multi-omic integration of miRNomic and lipidomic datasets was performed using the N-integration approach with the block.sPLS method from the mixOmics package (v.6.26.0) (5). The predictor matrix (X) included miRNA and lipid expression/abundance levels, while the response matrix (Y) was a dummy matrix encoding experimental groups based on AUD condition and sex. The model was fitted using three components with a fully connected design between blocks (design = "full"). To optimize feature selection, 20 features were retained for components 1 and 2, and 10 features for component 3 in X, while 6, 6, and 4 features were retained for components 1, 2, and 3 in Y, respectively. Further explorations of variable contributions and relationships across datasets used plotVar to visualize correlations and plotLoadings to identify key contributors within each dataset.

### Web Platform - *SexEVEthOmics*

In addition to the results presented in this article, an open-access, interactive web platform (https://carpercle.shinyapps.io/SexEVEthOmics/) was developed using the R shiny framework (v.1.10) (32). This tool enables users to access the full dataset and interactively explore differential miRNA expression results, functional analyses, lipidomic profiles, and multi-omics integration. The platform is structured into six sections and provides access to additional analyses and visualizations not included in the main manuscript. Some modules allow users to adjust parameters, offering opportunities for customized exploration and hypothesis generation.

## Results

### Sex-based Differences in the miRNA Expression Profile of AUD Patient Plasma EVs

To implement our knowledge in the search for biomarkers in plasma EVs from AUD patients, we analyzed plasma EV samples from female and male AUD and healthy patients (controls) who had been previously assessed via lipidomics (6). We investigated the role of miRNAs in the four experimental groups, defined by sex and chronic alcohol consumption, using miRNA-sequencing (miRNA-seq) data from corresponding plasma EV samples. DESeq2 identified differentially-expressed miRNAs between AUD and control samples within each sex (IF and IM comparisons). Figure 2A-B reports the upregulated (LFC > 0) and downregulated (LFC < 0) miRNAs (all results available on the web platform). We observed 4 upregulated and 3 downregulated miRNAs in females and 18 upregulated and 4 downregulated miRNAs in males. Notably, the comparison in males revealed a higher number of upregulated miRNAs compared to females (Figure 2A-B), suggesting distinct sex-specific responses to alcohol consumption. Notably, we failed to detect any significantly altered miRNAs in the IS comparison (Web Platform - Study Overview [https://carpercle.shinyapps.io/SexEVEthOmics/], Table S3).

We next validated miRNA-seq data using RT-qPCR (Figure 2C). We selected three miRNAs (*hsa-miR-194-5p*, *hsa-let-7b-5p*, and *hsa-miR-21-5p*) involved in the immune response (33–36), which revealed significant changes in AUD patients. Consistent with the miRNA-seq results, *hsa-miR-194-5p* and *hsa-miR-21-5p* tended to increase in AUD females compared to healthy females,

while *hsa-let-7b-5p* tended to decrease and *hsa-miR-21-5p* significantly increased in AUD males compared to healthy males. Overall, the data suggest that these miRNAs may participate in AUD pathogenesis in a sex-dependent manner.

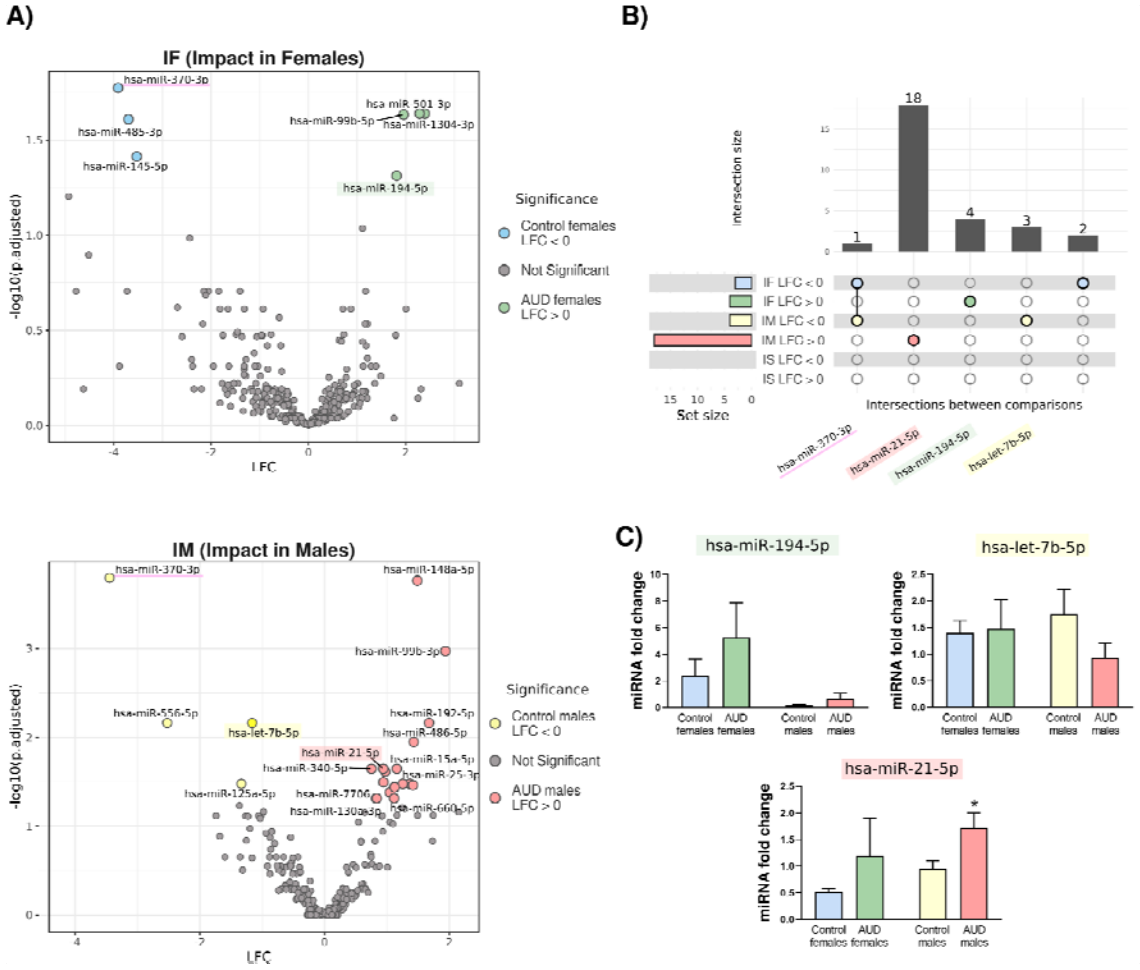


**Figure 2. Differential Expression and Validation of miRNAs in Plasma EVs from AUD and Control Patients Based on Sex. A)** Volcano plots demonstrate differential miRNA expression (adjusted p-value < 0.05) in the IF and IM comparisons. miRNAs with a positive log fold change (LFC > 0) display upregulation (green and red dots for IF and IM, respectively) and miRNAs with a negative LFC (LFC < 0) display downregulation (blue and yellow dots for IF and IM, respectively) in AUD patients. Highlighted miRNAs were validated by RT-qPCR, and underlined miRNA (hsa-miR-370-3p) represents common significantly altered miRNA between sexes. **B)** Intersection plot displaying shared and unique significantly altered miRNAs across IF, IM, and IS comparisons. miRNAs with names under the dots belong to that intersection pattern. **C)** RT-qPCR validation of three selected miRNAs: *hsa-miR-194-5p*, *hsa-let-7b-5p*, and *hsa-miR-21-5p*. Data represent mean ± SEM, n = 4-6 samples/group. * p < 0.05, compared to healthy controls. One-way ANOVA with Tukey multiple comparisons testing was performed. *AUD: alcohol use disorder, IF: AUD Impact in Females, IM: AUD Impact in Males, IS: Impact of Sex in AUD.*

**Sex-based Differences in miRNA Functional Analysis of Plasma EVs from AUD Patients**

We next assessed the functional impact of miRNA deregulation in AUD patient plasma EVs to provide biological insights into associated etiopathogenic pathways (37). We performed gene set analysis (GSA) on validated target genes associated with the differentially expressed miRNAs, incorporating GO terms related to Biological Processes (BP), Cellular Components (CC), and Molecular Functions (MF), and KEGG pathways. Notably, we observed several significantly impacted GO terms and KEGG pathways across IF, IM, and IS comparisons, highlighting notable sex-based differences. Table S4 summarizes the number of significant GSA results across the IF, IM, and IS comparisons, while Figures S2–S5 display the common significant results between IF and IM for the BP, CC, and MF ontologies. Figure 3A presents clusters derived from 66 common BP GO terms that exhibit significant sex-specific variation across all comparisons, characterized by negative LOR values in females and positive LOR values in males. These processes cluster into four main functional groups: (1) gene expression and protein turnover, encompassing ubiquitin-dependent degradation, mRNA regulation, splicing, phosphorylation, and catabolic pathways; (2) cell signaling and fate determination, such as cellular transformation, apoptosis, growth regulation, and receptor-mediated signaling; (3) cellular structure and stress response; and (4) vesicle-mediated transport related to intracellular trafficking and membrane dynamics.

Figure 3B illustrates a selection of the most relevant significantly altered GO terms characterized by distinct sex-dependent patterns. The MF ontology highlighted terms related to histone modifications, including histone H3 methylation and ubiquitin-related processes. The CC ontology revealed an enrichment in terms related to synaptic activity, including the pre- and post-synaptic regions, the axon, and EVs. Within the BP ontology, significant terms associated with neurological functions (e.g., axonogenesis and lipid metabolism), cellular communication, and vesicle-mediated transport, including Golgi-related pathways, Target of Rapamycin Complex 1 (TORC1) signaling, protein phosphorylation, and Mitogen-Activated Protein Kinase (MAPK) cascades. Interestingly, only terms associated with DNA replication - specifically, the BP term

"regulation of the DNA damage checkpoint" and the CC term "CMG complex" - exhibited a consistent pattern across IF and IM comparisons (Figures S2–S4).

Finally, KEGG pathway enrichment analysis revealed divergence between sexes in the functional impact of miRNA deregulation in AUD (Figure 3C). In AUD females (IF), several pathways displayed a negative LOR, whereas these pathways possessed a positive LOR in AUD males (IM). These pathways participate in a range of disease-related processes, including cancer-associated pathways linked to the excretory and digestive systems (e.g., renal cell carcinoma, bladder, pancreatic, and colorectal cancer), pathways related to cell signaling and growth regulation (e.g., mammalian target of rapamycin [mTOR], p53, and the family of receptor tyrosine kinases ErbB), immunity-related pathways, intracellular communication (e.g., axon guidance and adherens junctions), and metabolism and molecular processing associated with the endoplasmic reticulum. Figure S5 depicts results for the IS and C comparisons.

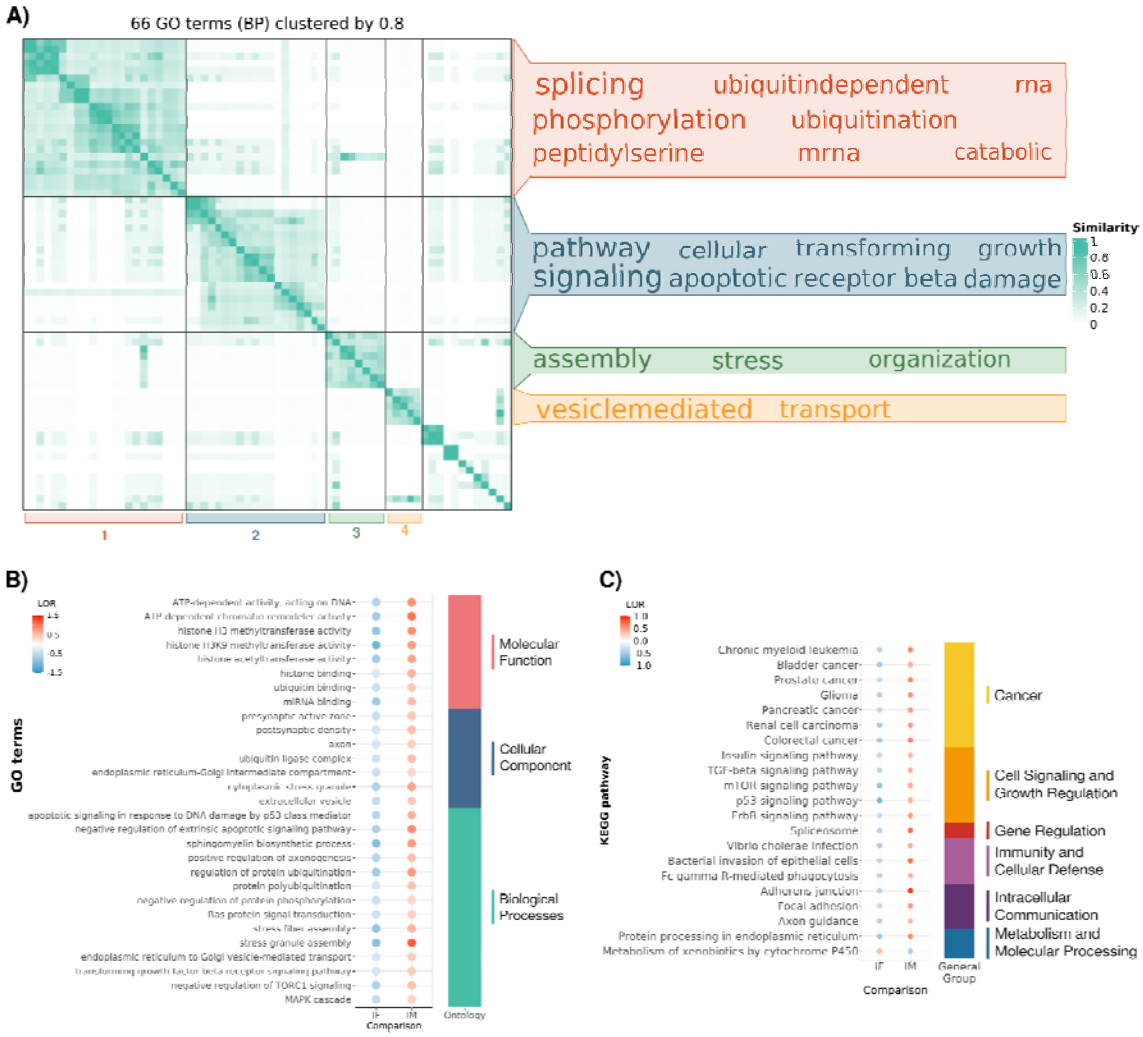


**Figure 3. Sex-Specific Functional Signatures of Plasma EV miRNAs in AUD Patients - Gene Set Analysis Results. A)** Clustering of significant BP GO terms common across IF, IM, and IS comparisons based on semantic similarity (threshold ≥ 0.8). Word clouds summarize representative terms for each cluster. **B)** Dot plot depicting selected significant GO terms (absolute LOR > 0.3) across MF, CC, and BP ontologies. Dot color represents the LOR value, and the right-side color bars indicate the ontology category of each term. **C)** Dot plot illustrating significant KEGG pathways (absolute LOR > 0.3). Dot color represents the LOR value, while the right-side color bars classify pathways into general functional groups. *AUD: alcohol use disorder, BP: Biological Processes, CC: Cellular components, IF: AUD Impact in Females, IM: AUD Impact in Males, GO: Gene Ontology, KEGG: Kyoto Encyclopedia of Genes and Genomes, LOR: log odds ratio, MF: Molecular Functions.*

## Integrated Transcriptomic and Lipidomic Analyses Reveal Sex-based Differences in AUD Patient Plasma EVs

We employed our miRNomic data, combined with lipidomics data from Perpiñá-Clerigués et al. (6), to explore novel relationships between miRNAs and lipids in plasma EVs isolated from AUD

females and males, thereby generating new hypotheses to explain the mutual relationships between these variables. After data preprocessing and normalization according to their respective omic natures, we obtained a total of 387 miRNAs and 575 lipids for the same samples. Figure S6 illustrates the sPLS results, where the samples exhibit comparable spatial organization in both datasets, with high correlation values observed for the first two components (Comp1: 0.951 and Comp2: 0.953). This strong alignment suggests the successful application of the N-integration methodology (block.sPLS).

***Biological Patterns Captured by Components 1 and 2: Links to Alcohol Consumption and Sex***

Performing dimension reduction using the mixOmics package produces latent components defined by their loading vectors, which indicate the weight of each original variable's contribution to the component. Figure 4 depicts the sample plot and the loadings plot for Components 1 and 2. Component 1 captures variance related to alcohol consumption, while Component 2 captures variance related to sex. The bar plots display the loading values, indicating the extent to which each feature contributes to the differentiation of the groups; those at the bottom and those with longer bars have the most significant influence. As a result, we identified a subset of 40 miRNAs (Figure 4B) and 40 lipids (Figure 4C) that may distinguish and clarify the influence of alcohol (e.g., hsa-miR-148a-5p, hsa-miR-7706, and hsa-miR-21-5p and Cer_NDS d39:1_neg, EtherPC 16:0e_18:2_neg, and SM d18:2_23:0) and sex (e.g., hsa-miR-30d-5p, hsa-miR-152-3p, and hsa-miR-1271-5p and Cer_NDS d39:1_neg, EtherPC 16:0e_18:2_neg, and SM d18:2_23:0). Table S5 details the description of lipid subclass abbreviations.

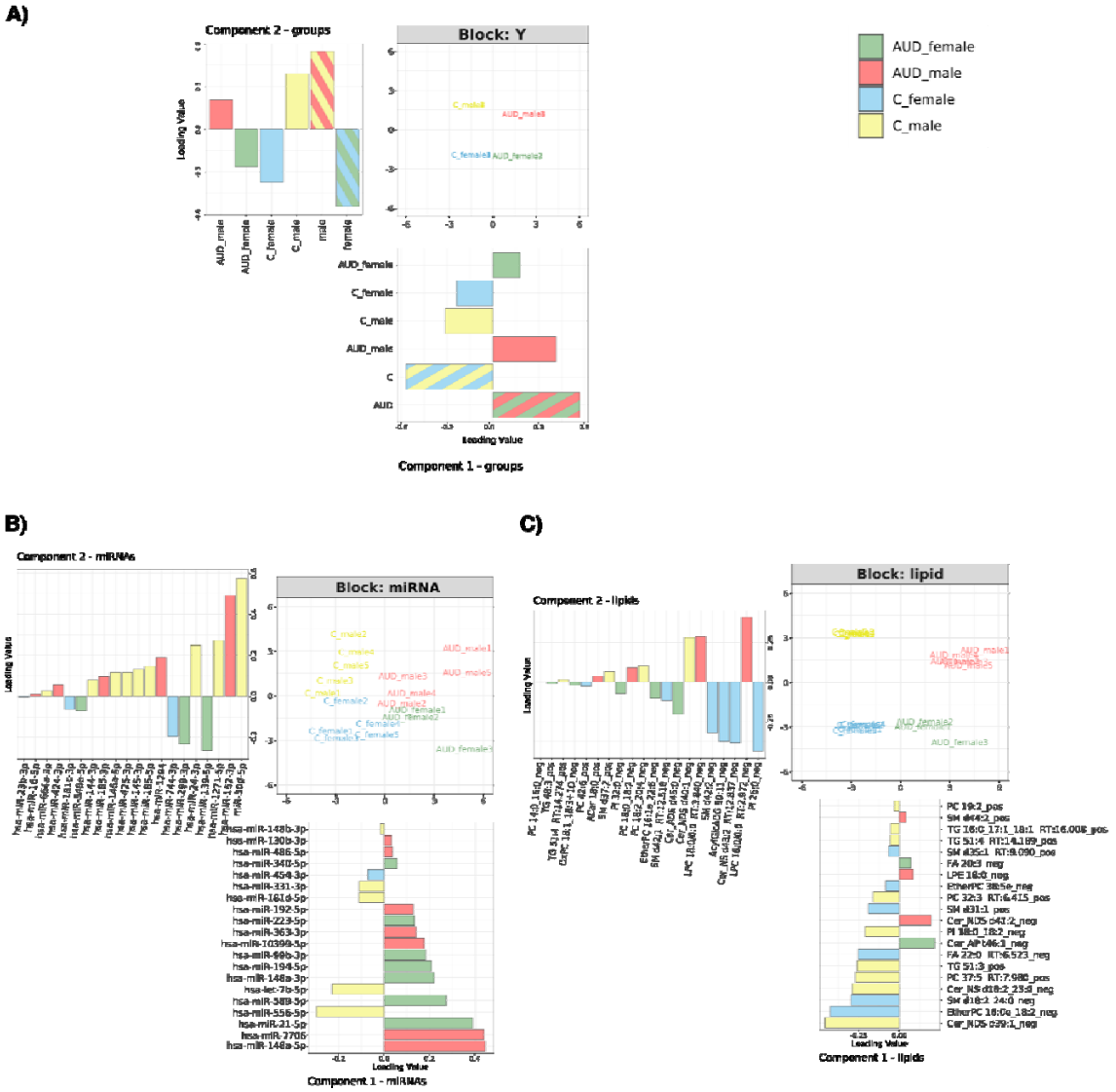


**Figure 4. AUD- and Sex-driven Sample Separation Based on Integrated Patient EV miRNA and Lipid Profiles.** Sample and loading plots from the block.sPLS integration analysis performed using mixOmics, representing Components 1 and 2. Samples are projected into the space defined by the components derived from the (**A**) metadata (Y), (**B**) miRNA, and (**C**) lipid dataset. The loading plots identify the most relevant variables contributing to each component: (**A**) metadata (Y), (**B**) miRNA, and (**C**) lipids. Component 1 is represented on the X-axis, with its corresponding loading plot displayed behind the sample plot. Component 2 is shown on the Y-axis, with its loading plot displayed to the left. Colors in the sample plots indicate the experimental groups. Colors in the loading plots denote which experimental group has the highest mean expression/abundance of that feature.

A correlation plot with a cutoff of 0.5 illustrated the relationship between the miRNomic and lipidomic datasets and the experimental groups (Figure 5). In line with our focus on integrating these molecular features into a comprehensive physiological and pathological framework, Figure 5

highlights those lipids and miRNAs associated with pathologies/terms related to alcohol consumption (Table S6 provides more detailed information). The features positioned in the upper and lower areas associate with males and females, respectively, while the features on the right and left sides correspond to AUD and control patients, respectively.

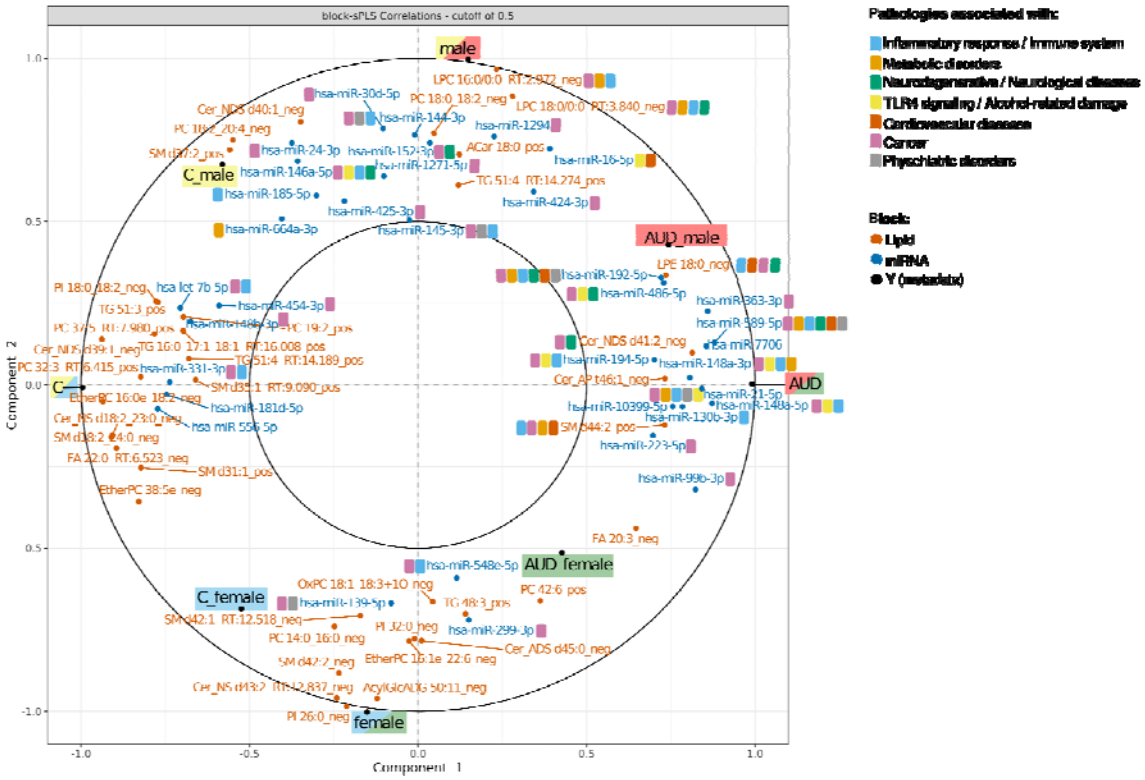


**Figure 5. Integrated Lipid–miRNA Correlation Map Reveals Sex- and AUD-specific Molecular Patterns.** Varplot from the block.sPLS analysis displaying Component 1 vs. Component 2 (cutoff = 0.5). The plot displays the correlations between selected variables from the miRNA and lipidomic blocks and the experimental groups (Y block), projected onto the first two components. Only variables with a correlation ≥ |0.5| are shown. Labels are colored by block (lipid, miRNA, or Y), and icons indicate the associated pathologies based on literature annotation. Sample group centroids are highlighted (e.g., AUD female, control male), and distribution patterns reveal distinct molecular signatures by sex and alcohol exposure.

Table 1 presents the AUD signature of 20 miRNAs and 20 lipids identified through the integrated joint model that maximizes the separation between AUD patients and controls. This multivariate panel effectively captured the combined discriminative power of both molecular layers; additionally, by integrating results from univariate linear regression analyses (DEA: Differential expression analysis of miRNome data, DAA: Differential abundance analysis of lipidome data), we highlighted the miRNAs and lipids that individually differentiate the experimental groups in at least

one sex. We consider that these features contribute additional robustness to the panel, representing potential biomarkers with strong discriminative capacity (relevant in a sex-specific context).

**Table 1. AUD Signature Based on Multi-omics Integration (Component 1).**

| FEATURE | PATTERN | DEA/DAA | FEATURE | PATTERN | DEA/DAA |
|---|---|---|---|---|---|
| Cer_AP t46:1_neg | + | F | Cer_NS d18:2_23:0_neg | - | F & M |
| Cer_NDS d41:2_neg | + | | EtherPC 16:0e_18:2_neg | - | F & M |
| FA 20:3_neg | + | M | EtherPC 38:5e_neg | - | M |
| LPE 18:0_neg | + | | FA 22:0 RT:6.523_neg | - | |
| SM d44:2_pos | + | | PC 19:2_pos | - | M |
| hsa-miR-10399-5p | + | M | PC 32:3 RT:6.415_pos | - | |
| hsa-miR-130b-3p | + | | PC 37:5 RT:7.980_pos | - | |
| hsa-miR-148a-3p | + | M | PI 18:0_18:2_neg | - | M |
| hsa-miR-148a-5p | + | M | SM d18:2_24:0_neg | - | F & M |
| hsa-miR-192-5p | + | M | SM d31:1_pos | - | |
| hsa-miR-194-5p | + | F | SM d35:1 RT:9.090_pos | - | |
| hsa-miR-21-5p | + | M | TG 16:0_17:1_18:1 RT:16.008_pos | - | |
| hsa-miR-223-5p | + | | TG 51:3_pos | - | |
| hsa-miR-340-5p | + | M | TG 51:4 RT:14.189_pos | - | |
| hsa-miR-363-3p | + | M | hsa-let-7b-5p | - | M |
| hsa-miR-486-5p | + | M | hsa-miR-148b-3p | - | |
| hsa-miR-589-5p | + | | hsa-miR-181d-5p | - | |
| hsa-miR-7706 | + | M | hsa-miR-331-3p | - | |

| | | |
|---|---|---|
| hsa-miR-99b-3p | + | M |

| | | |
|---|---|---|
| hsa-miR-454-3p | - | |
| hsa-miR-556-5p | - | M |

This panel includes 40 features (lipids and miRNAs) identified through block.sPLS. Positive (+) or negative (-) symbols indicate the correlation of the feature with the AUD condition. DEA/DAA column indicates the sex where the feature presented a statistical significance in the individual regression analyses. *AUD: Alcohol use disorder, DEA: Differential Expression Analysis of miRNome, DAA: Differential Abundance Analysis of lipidome / M: male, F: female.*

***Divergent Patterns Based on AUD and Sex Captured by Component 3***

Figure 6A displays the loading plots for Component 3, highlighting opposing patterns between the main experimental groups and a set of 10 miRNAs and 10 lipids that explain the variance in this component. Figure 6B-C presents the mean values of these variables to visualize miRNA expression and lipid abundance patterns across the experimental groups. Three main patterns emerge from these results: (I) the pattern in light gray indicates an increase in AUD females and a decrease in AUD males compared to controls (e.g., hsa-miR-1301-3p and Cer_NS d18:1_24:1) (Figure S1-A1); (II) the pattern in dark gray indicates a decrease in AUD females and an increase in AUD males relative to controls (e.g., hsa-miR-1260b and Cer_NS d18:1_22:0) (Figure S1-B6); and (III) the pattern in white indicates stability when comparing controls of both sexes, with a specific variation (increase or decrease) in one sex within AUD patients relative to its corresponding control (e.g., hsa-miR-197-3p) (Figure S1-A2, -B7, and B9). Patterns I and II exhibit an apparent cross-over effect, as the response to AUD follows an opposing trend between sexes, with increases in one sex corresponding to decreases in the other. These patterns suggest a sex-dependent response to AUD, where specific miRNAs and lipids exhibit opposite expression trends between males and females. Notably, we found that specific lipids identified in these patterns displayed significance or a trend towards significance in the individual analysis for the IS comparison (Figure 1), reinforcing the impact of sex on the impact of AUD. In contrast, the transcriptomics analysis failed to reveal significant results for the IS comparison (Figure 2); however, a set of miRNAs emerged through the integrative approach, highlighting the influence of sex in AUD. Table 2 summarizes the AUD-sex signature.

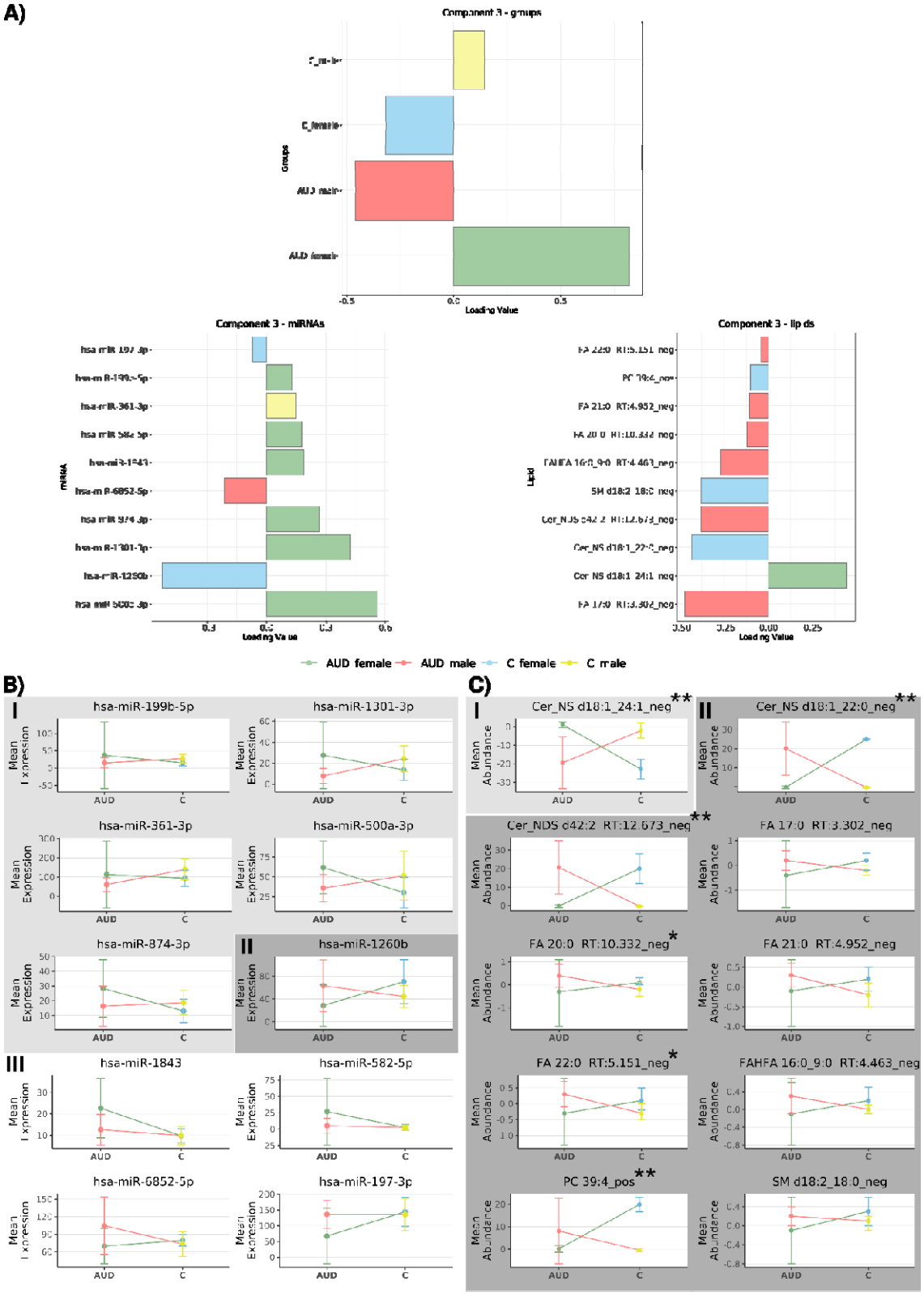
A)
Component 3 - groups
Groups
Loading Value
Component 3 - miRNAs
miRNA
Loading Value
Component 3 - lipids
Lipid
Loading Value
AUD female
AUD male
C female
C male
B)
I
hsa-miR-199b-5p
hsa-miR-1301-3p
hsa-miR-361-3p
hsa-miR-500a-3p
hsa-miR-874-3p
II
hsa-miR-1260b
III
hsa-miR-1843
hsa-miR-582-5p
hsa-miR-6852-5p
hsa-miR-197-3p
Mean Expression
AUD
C
C)
I
Cer_NS d18:1_24:1_neg **
II
Cer_NS d18:1_22:0_neg **
Cer_NDS d42:2_RT:12.673_neg **
FA 17:0_RT:3.302_neg
FA 20:0_RT:10.332_neg *
FA 21:0_RT:4.952_neg
FA 22:0_RT:5.151_neg *
FAHFA 16:0_9:0_RT:4.463_neg
PC 39:4_pos **
SM d18:2_18:0_neg
Mean Abundance
AUD
C

**Figure 6. AUD-Sex Signature Reveals Divergent Patterns by Sex and AUD Status. A)** Loading plot from block.sPLS integration for Component 3. **B)** Mean expression levels of miRNAs and **C**) mean abundance of lipids that explain the variance in Component 3 across experimental groups. *denotes a trend (0.05 < adjusted p-value < 0.055) and **denotes statistical significance (adjusted p-value < 0.01) in the regression analysis (IS comparison of differential expression/abundance analysis). Background colors (light grey, dark grey, and white) indicate the patterns I, II, and III.

**Table 2. AUD-Sex Signature Based on Multi-omics Integration (Component 3)**

| FEATURE | PATTERN | DEA |
|---|---|---|
| hsa-miR-1301-3p | I | |
| hsa-miR-199b-5p | I | |
| hsa-miR-361-3p | I | |
| hsa-miR-500a-3p | I | |
| hsa-miR-874-3p | I | |
| hsa-miR-1260b | II | |
| hsa-miR-1843 | III | |
| hsa-miR-197-3p | III | |
| hsa-miR-582-5p | III | |
| hsa-miR-6852-5p | III | |

| FEATURE | PATTERN | DAA |
|---|---|---|
| Cer_NS d18:1_24:1_neg | I | x |
| Cer_NS d18:1_22:0_neg | II | x |
| Cer_NDS d42:2 RT:12.673_neg | II | x |
| FA 17:0 RT:3.302_neg | II | |
| FA 20:0 RT:10.332_neg | II | # |
| FA 21:0 RT:4.952_neg | II | |
| FA 22:0 RT:5.151_neg | II | # |
| FAHFA 16:0_9:0 RT:4.463_neg | II | |
| PC 39:4_ pos | II | x |
| SM d18:2_18:0_neg | II | |

| | |
|---|---|
| I | AUD_Female, C_Male |
| II | AUD_Male, C_Female |
| III | One sex remains stable |

This panel includes 20 features (lipids and miRNAs) identified through block.sPLS. The pattern indicates the group where the feature is higher in each sex (AUD or Control group). X in the DEA and DAA columns indicates statistical significance (adjusted p-value < 0.01) in the IS comparison in the individual regression analyses (DEA/DAA); # denotes a trend towards significance (0.05 < adjusted p-value < 0.055). *AUD: Alcohol Use Disorder, DEA: Differential Expression Analysis of miRNome, DAA: Differential Abundance Analysis of lipidome, F: female, M: male, IS: Impact of Sex Comparison.*

### *SexEVEthOmics*

We made all results accessible through the interactive *SexEVEthOmics* web platform [https://carpercle.shinyapps.io/SexEVEthOmics], which includes additional analyses beyond those discussed in the manuscript.

## Discussion

Multi-omics data integration enables the connection of biological information across distinct molecular layers (e.g., lipids, transcripts, proteins), offering a more holistic perspective on physiological alterations (38). Integrative multivariate methods enable the identification of molecular signatures that emerge from the coordinated contributions of multiple variables. This capacity to detect biologically meaningful combinations enhances the potential of multi-omics integration for discovering robust diagnostic or prognostic signatures in complex conditions such as AUD, particularly when explored with a focus on EV cargo.

While lipidomic or miRNomic analyses of EVs have been previously applied to the study of AUD (6,39), this study, to the best of our knowledge, represents the first to implement a multi-omics integration of both omic layers, providing a more comprehensive molecular perspective of AUD. The analysis of EVs identified distinct molecular signatures composed of specific combinations of highly correlated miRNAs and lipids. Our multivariate approach yielded two miRNA-lipid signatures: 1) the AUD signature, comprising a set of 40 biomarkers (20 miRNAs and 20 lipids) that differentiate individuals with AUD from controls; and 2) the AUD-sex signature, consisting of 20 biomarkers (10

miRNAs and 10 lipids) that highlight sex-based differences in the impact of AUD. Our data implicate the integrated features (Tables 1 and 2) in alcohol-related pathophysiological processes and effectively discriminate individuals with AUD from healthy individuals, including sex-specific response to AUD. Importantly, we chose these variables not for their predictive strength, but for their collective contribution to maximizing group separation in the multivariate space when applying the block.sPLS model. This approach highlights a crucial feature of integrative multivariate models: some features may be weak or non-significant when assessed independently, but can become highly informative when considered in combination as part of a coordinated molecular signature. Prior to integration, we performed univariate differential analyses of lipidomic (6) and miRNomic datasets to identify individual features associated with AUD and sex. These analyses allowed us to explore potential biomarkers with strong individual effects and characterize group- and sex-specific expression patterns in each distinct molecular layer. In the context of miRNomics, we identified 7 (females) and 16 (males) significantly altered miRNAs, with only one miRNA in common. These overlapping features offer additional robustness, suggesting sex-specific biomarker candidates with potentially greater individual effect sizes (e.g., hsa-miR-99b-3p). The RT-qPCR validation of hsa-let-7b-5p, hsa-miR-194-5p, and hsa-miR-21-5p confirmed the direction of the significant bioinformatics results. In our study, hsa-let-7b-5p displayed downregulation in AUD males; this same miRNA was reported by Wang et al. (39), in a study that profiled miRNAs from plasma small EVs exclusively in AUD males. Significantly, the *Let-7* miRNA family contributes to hippocampal neurodegeneration and has been implicated in alcoholism-addiction (39,40) while ethanol can trigger neuroimmune responses involving the release of *let-7b*/*HMGB1* complexes via microglia-derived microvesicles (41). We also observed the upregulated expression of hsa-miR-194-5p in AUD females; related studies also reported significantly higher hsa-miR-194-5p expression in plasma neuron-derived EVs from young individuals with high alcohol consumption (33) and in the frontal cortex of alcoholic patients (34). This miRNA has also been implicated in hepatocarcinoma and the regulation of the nuclear factor kappa-light-chain-enhancer of activated B cells (NF-κB) pathway (42). Moreover, we also observed the upregulation of hsa-miR-21-5p expression in DEA and RT-qPCR validation

associated with AUD in both sexes. This miRNA has been implicated in inflammatory immune processes by modulating the Interleukin 6 receptor (IL6R) and signal transducer and activator of transcription 3 (STAT3) pathway in microglia (43) and alcohol-related liver disease (44). While differential hsa-miR-21-5p expression has been observed in plasma EVs from ethanol-intoxicated adolescents of both sexes (35), such variation aligns with known disparities between acute and chronic alcohol use (40).

AUD exerts complex biological effects, increasing the risk of cardiovascular, neurological, metabolic, hepatic, and oncological diseases (45,46). Although we possess data regarding sex-based differences in AUD, particularly in inflammatory responses (47,48), they are frequently overlooked in research. The historic underrepresentation of females in AUD studies has resulted in critical gaps in understanding, diagnosis, and treatment, which may contribute to poorer clinical outcomes and underscore the urgent need for more inclusive and sex-informed research and therapeutic strategies (49). Incorporating sex as a biological variable remains essential to developing targeted and effective treatments (47). In our study, we identified sex-specific miRNomic and lipidomic signatures associated with alcohol-induced molecular alterations, including divergent functional responses to ethanol exposure. Several affected pathways related to inflammation, autophagy, and cellular stress, representing processes commonly implicated in alcohol-related pathologies and cancer. Among the seven cancer-related KEGG pathways identified, we observed the recurrent involvement of crucial genes (e.g., *MAP2K1*, *BRAF*, *KRAS*, *MAPK3*, *ARAF*, *RAF1*, and *MAPK1*) frequently mutated or dysregulated in cancer that play central roles in tumor progression by promoting proliferation, survival, invasion, and metastasis through activation of the MAPK/ERK signaling cascade (50). Interestingly, differentially expressed miRNAs predicted to target these oncogenes exhibited marked sex specificity, with only one miRNA shared between males and females. This sex-dependent regulatory pattern may reflect distinct molecular adaptations to chronic alcohol exposure and could contribute to differential cancer susceptibility and progression. Notably, several features from the AUD–sex signature have previously been associated with cancer in other contexts; for example, hsa-miR-1260b has been implicated in pancreatic, lung, ovarian, breast, and myxofibrosarcoma cancers

(51–55).

Our data also revealed pronounced sex-specific alterations in autophagy-related regulatory pathways, including those mediated by p53, ubiquitination, Transforming Growth Factor beta (TGF-β), TORC1, the MAPK cascade, mTOR, ErbB signaling, and histone H3 methylation. Prior studies underscored the importance of autophagy in responses to substance-induced stress, particularly alcohol exposure (56–58) and alcohol-associated pathologies such as hepatotoxicity (59). For instance, alcohol triggers p53-mediated apoptosis in neural crest cells by suppressing TORC1 activity and ribosomal biogenesis, illustrating the complex interplay of these pathways in alcohol-induced neurotoxicity (60). Chronic alcohol intake also inhibits autophagy and enhances apoptosis in hepatic tissue (61); moreover, several reports documented sex-based differences in autophagy regulation (62,63), which may help to explain the divergent responses observed in our data in AUD. These differences may contribute to varying susceptibilities to alcohol-induced organ damage and have important implications for the development of sex-informed therapeutic strategies targeting autophagy. These sex-dependent molecular patterns extended to oxidative stress responses as well. Although evidence suggests that males are generally more susceptible to oxidative damage and chronic inflammation, whereas females—particularly before menopause—tend to exhibit stronger inflammatory responses and enhanced antioxidant capacity (64), women are generally more susceptible to developing liver disease or cardiomyopathy after consuming alcohol than men, as well as having a higher incidence of depression and anxiety (65). Although direct evidence for sex-specific stress granule responses to chronic alcohol exposure is limited, cytoplasmic stress granule formation has been reported in *Saccharomyces cerevisiae* under ethanol stress (66), and sex differences in stress granule composition have been documented in murine models during cold exposure (67). Our data revealed a divergent expression pattern consistent with sex-specific regulation of stress granules, and one miRNA from our AUD–Sex signature, hsa-miR-197-3p, has been linked to exosomal miRNAs in depression (68) and to circulating miRNAs associated with endothelial dysfunction and cardiometabolic risk in conditions such as Kawasaki disease (69).

Finally, the sphingomyelin biosynthetic process emerged in our sex-differential analysis, reinforcing the notion of sex-specific regulation of sphingolipid metabolism in alcohol-induced brain alterations. This finding agrees with previous reports describing sexual dimorphism in white matter vulnerability and behavioral outcomes in AUD patients (70). Our previous studies highlighted the role of acid sphingomyelinase in modulating emotional phenotypes and an association with sex-related comorbidities such as depression and anxiety in AUD (6); moreover, a lipid-driven mechanism involving sphingomyelinases and mitochondria-associated endoplasmic reticulum membranes has been implicated in ethanol-induced EV secretion in glial cells (71). Our current findings support the hypothesis that sex-specific activity in sphingolipid pathways contributes to divergent neurobiological trajectories in males and females following chronic alcohol exposure. Furthermore, recent evidence has revealed that ceramide production via neutral sphingomyelinase 2 regulates exosomal miRNA secretion and that inhibiting this pathway reduces exosome formation (72,73), a process that also appears to be modulated by sex.Multivariate analysis proved particularly valuable for uncovering sex-related differences in disease mechanisms by capturing complex expression patterns that remained undetected in univariate comparisons (70). While the differential expression analysis of the miRNomic data failed to reveal any significant alterations in the sex-based (IS) comparison at the individual variable level, the integrative multi-omic analysis uncovered a subset of sex-associated miRNAs, underscoring the influence of sex in AUD when analyzing distinct omic layers together. Notably, Component 3 revealed a distinct AUD–sex signature, suggesting that sex-based differences in AUD may not only arise from differences in magnitude but also from qualitatively distinct expression profiles (e.g., upregulation in one sex and stable expression in the other). Additionally, this integrative strategy provided complementary evidence that reinforced findings from the univariate analysis; specifically, 6 of 10 lipids contributing to Component 3 also displayed significance or consistent trends in the individual lipidomic IS analysis (6). These lipids belong to classes previously associated with male sex, inflammation, and hepatotoxicity, including ceramides (Cer), sphingomyelins (SM), and fatty acids (FA). Moreover, a substantial proportion of the 40 lipids contributing to AUD- and sex-based separations in Components 1 and 2 overlapped with the most

deregulated species identified in the univariate analyses, particularly lysophosphatidylcholines (LPC), phosphatidylcholines (PC), sphingomyelins (SM), and ceramides (Cer).

As emerging disciplines, multi-omics and EV analysis represent the forefront of scientific innovation; however, they still face several limitations. The limited number of plasma samples from AUD females represents a significant limitation of this study; women often do not underreport alcohol-related problems and this issue in women tends to be overlooked in primary care and other settings (74). Another limitation arises from integrating multi-omics data from the same individuals, which commonly results in the loss of samples due to missing data across omic layers. While newer methodologies can mitigate this problem, the challenge remains a significant limitation in multi-omics-based studies (75). Although integration enhances class discrimination, this approach does not establish direct links between transcripts and metabolites, which limits the potential for deeper biological interpretation due to the inherent differences between distinct omic layers (76). Furthermore, the lack of a consensual optimal miRNA normalization strategy highlights the difficulty in comparing studies (77).

## Conclusions

The evolution of omic-based technologies has been accompanied by parallel advances in data analysis strategies, enabling researchers to extract deeper insights from increasingly complex datasets. In this study, we employed complementary approaches, including individual and integrative analyses with multifaceted hypotheses, to lay the groundwork for future strategies aimed at enhancing our understanding of AUD, a condition that intersects with numerous other diseases and carries both biological and social implications. Therefore, we propose: (1) an AUD signature for predictive modeling, which could contribute to both prognostic and diagnostic applications, (2) an AUD-sex signature to capture sex-specific molecular biomarkers, enabling a deeper understanding of how biological responses to alcohol differ between females and males. This latter aspect contributes to reducing the persistent gap in female representation within alcohol-related research. Together, our findings support the identification of biologically grounded and sex-informed molecular patterns with potential translational value, which can ultimately be translated into non-invasive biomarker panels to

enhance the detection, monitoring, and personalized intervention strategies for AUD. Overall, these findings indicate that both alcohol exposure and biological sex leave measurable imprints on EV cargos, reinforce the value of incorporating sex as a critical variable in AUD research, and underscore the power of multi-omics integration as a key strategy for investigating complex biological systems.

## Declarations

### Ethics approval and consent to participate

Human plasma samples were used in accordance with the Declaration of Helsinki and were approved by the Ethics Committee of the University Hospital of Salamanca (March 2010). Written informed consent was obtained from each participant.

### Consent for publication

Not applicable

### Availability of data and materials

The normalized and analyzed datasets, along with the programming scripts, are available in the GitHub repository https://github.com/carlapercle/SexEVEthOmics and through the interactive web platform https://carpercle.shinyapps.io/SexEVEthOmics/. The small RNA-seq data have been deposited in the NCBI Sequence Read Archive (SRA) under accession number PRJNA1291119 .

### Competing interests

The authors declare no competing interests

### Funding

This work has been supported by grants from the Spanish Ministry of Health□PNSD (2019□I039, 2023-I024), GVA (CIAICO/2021/203), GVA (CIAICO/2023/149), the Carlos III Institute, and the Primary Addiction Care Research Network (RD21/0009/0005, RD24/0003/0017), FEDER Funds, GVA and the Instituto de Salud Carlos III (ISCIII) through projects PI10/01692 and PI20/00743, co-funded by the European Union and the Junta de Castilla y León (GRS 2648/A/22), PID2023-146865OB-I00 and PID2021-124430OA-I00 funded by MCIN/AEI/10.13039/501100011033/FEDER, UE ("A way to make Europe"), and partially funded by the Institute of Health Carlos III (project IMPaCT-Data, exp. IMP/00019), co-funded by the European

Union, European Regional Development Fund (ERDF, "A way to make Europe"). C. Perpiñá-Clérigues was supported by a predoctoral fellowship (ACIF/2021/338) and internship grant (CIBEFP/2023/106) from the Generalitat Valenciana.

**Authors' contributions**

CPC analyzed the data; MP and FGG designed and supervised the bioinformatics analysis; SK and KL guided in the multi-omics approach; MFR and MM obtained human plasma samples; SM isolated EVs from human plasma; CPC and BMU designed and implemented the web tool; CPC, MP, FGG and CGR wrote the manuscript; SM and CPC designed the graphical abstract; CPC, MP, FGG and CGR helped in the interpretation of the results; CPC, CGR, MM, MP and FGG writing-review and editing; MP and FGG conceived the work. All authors read and approved the final manuscript.

**Acknowledgments**

The authors thank the Príncipe Felipe Research Center (CIPF) for providing access to the cluster, which is co-funded by the European Regional Development Fund (FEDER) in the Valencian Community (2014-2020). The authors also thank the Genomics and Genetics Service at the Príncipe Felipe Research Centre and Stuart P. Atkinson for reviewing the manuscript.

## References

1. Babu M, Snyder M (2023): Multi-Omics Profiling for Health. *Mol Cell Proteomics* 22: 100561.
2. Ma P, Wang Z, Wang Y, Hou B, Sun J, Tian H, *et al.* (2021): Integration of Metabolomics and Transcriptomics Reveals Ketone Body and Lipid Metabolism Disturbance Related to ER Stress in the Liver. *J Proteome Res* 20: 3875–3888.
3. Tarazona S, Arzalluz-Luque A, Conesa A (2021): Undisclosed, unmet and neglected challenges in multi-omics studies. *Nat Comput Sci* 1: 395–402.
4. Maan K, Baghel R, Dhariwal S, Sharma A, Bakhshi R, Rana P (2023): Metabolomics and transcriptomics based multi-omics integration reveals radiation-induced altered pathway networking and underlying mechanism. *Npj Syst Biol Appl* 9: 42.
5. Rohart F, Gautier B, Singh A, Lê Cao K-A (2017): mixOmics: An R package for ‘omics feature selection and multiple data integration ((D. Schneidman, editor)). *PLOS Comput Biol* 13: e1005752.
6. Perpiñá-Clérigues C, Mellado S, Galiana-Roselló C, Fernández-Regueras M, Marcos M, García-García F, Pascual M (2024): Novel insight into the lipid network of plasma extracellular

vesicles reveal sex-based differences in the lipidomic profile of alcohol use disorder patients. *Biol Sex Differ* 15: 10.

7. Lim Y, Beane-Ebel JE, Tanaka Y, Ning B, Husted CR, Henderson DC, *et al.* (2021): Exploration of alcohol use disorder-associated brain miRNA–mRNA regulatory networks. *Transl Psychiatry* 11: 504.
8. Hitzemann R, Bergeson SE, Berman AE, Bubier JA, Chesler EJ, Finn DA, *et al.* (2022): Sex Differences in the Brain Transcriptome Related to Alcohol Effects and Alcohol Use Disorder. *Biol Psychiatry* 91: 43–52.
9. Geneva: World Health Organization (2024): *Global Status Report on Alcohol and Health and Treatment of Substance Use Disorders.* Retrieved from https://iris.who.int/bitstream/handle/10665/377960/9789240096745-eng.pdf?sequence=1
10. Mostafa H, Amin AM, Teh C-H, Murugaiyah VA, Arif NH, Ibrahim B (2017): Plasma metabolic biomarkers for discriminating individuals with alcohol use disorders from social drinkers and alcohol-naive subjects. *J Subst Abuse Treat* 77: 1–5.
11. Clayton A, Harris CL, Court J, Mason MD, Morgan BP (2003): Antigen□presenting cell exosomes are protected from complement□mediated lysis by expression of CD55 and CD59. *Eur J Immunol* 33: 522–531.
12. Yuan Y, Sun J, You T, Shen W, Xu W, Dong Q, Cui M (2022): Extracellular Vesicle-Based Therapeutics in Neurological Disorders. *Pharmaceutics* 14: 2652.
13. Donoso□Quezada J, Ayala□Mar S, González□Valdez J (2021): The role of lipids in exosome biology and intercellular communication: Function, analytics and applications. *Traffic* 22: 204–220.
14. Su H, Rustam YH, Masters CL, Makalic E, McLean CA, Hill AF, *et al.* (2021): Characterization of brain□derived extracellular vesicle lipids in Alzheimer's disease. *J Extracell Vesicles* 10: e12089.
15. Fernández-Regueras M, Carbonell C, Salete-Granado D, García J-L, Gragera M, Pérez-Nieto M-Á, *et al.* (2023): Predominantly Pro-Inflammatory Phenotype with Mixed M1/M2 Polarization of Peripheral Blood Classical Monocytes and Monocyte-Derived Macrophages among Patients with Excessive Ethanol Intake. *Antioxidants* 12: 1708.
16. R Development Core Team (n.d.): *R: A Language and Environment for Statistical Computing.* Vienna: R Foundation for Statistical Computing. Retrieved from https://www.r-project.org/
17. Ibáñez F, Montesinos J, Ureña-Peralta JR, Guerri C, Pascual M (2019): TLR4 participates in the transmission of ethanol-induced neuroinflammation via astrocyte-derived extracellular vesicles. *J Neuroinflammation* 16: 136.
18. Callahan BJ, McMurdie PJ, Rosen MJ, Han AW, Johnson AJA, Holmes SP (2016): DADA2: High-resolution sample inference from Illumina amplicon data. *Nat Methods* 13: 581–583.

19. Martin M (2011): Cutadapt removes adapter sequences from high-throughput sequencing reads. *EMBnet.journal* 17: 10.

20. Langmead B, Salzberg SL (2012): Fast gapped-read alignment with Bowtie 2. *Nat Methods* 9: 357–359.

21. Griffiths-Jones S (2006): miRBase: microRNA sequences, targets and gene nomenclature. *Nucleic Acids Res* 34: D140–D144.

22. Locati MD, Terpstra I, de Leeuw WC, Kuzak M, Rauwerda H, Ensink WA, *et al.* (2015): Improving small RNA-seq by using a synthetic spike-in set for size-range quality control together with a set for data normalization. *Nucleic Acids Res* 43: e89–e89.

23. Love MI, Huber W, Anders S (2014): Moderated estimation of fold change and dispersion for RNA-seq data with DESeq2. *Genome Biol* 15: 550.

24. Benjamini Y, Hochberg Y (1995): Controlling the False Discovery Rate: A Practical and Powerful Approach to Multiple Testing. *J R Stat Soc Ser B Methodol* 57: 289–300.

25. Skoufos G, Kakoulidis P, Tastsoglou S, Zacharopoulou E, Kotsira V, Miliotis M, *et al.* (2024): TarBase-v9.0 extends experimentally supported miRNA–gene interactions to cell-types and virally encoded miRNAs. *Nucleic Acids Res* 52: D304–D310.

26. Cui S, Yu S, Huang H-Y, Lin Y-C-D, Huang Y, Zhang B, *et al.* (2025): miRTarBase 2025: updates to the collection of experimentally validated microRNA–target interactions. *Nucleic Acids Res* 53: D147–D156.

27. Montaner D, Dopazo J (2010): Multidimensional Gene Set Analysis of Genomic Data ((J. Hoheisel, editor)). *PLoS ONE* 5: e10348.

28. Ashburner M, Ball CA, Blake JA, Botstein D, Butler H, Cherry JM, *et al.* (2000): Gene Ontology: tool for the unification of biology. *Nat Genet* 25: 25–29.

29. Kanehisa M (2004): The KEGG resource for deciphering the genome. *Nucleic Acids Res* 32: 277D – 280.

30. Carlson M (2017): org.Hs.eg.db. Bioconductor. https://doi.org/10.18129/B9.BIOC.ORG.HS.EG.DB

31. Gu Z, Hübschmann D (2023): *SimplifyEnrichment*: A Bioconductor Package for Clustering and Visualizing Functional Enrichment Results. *Genomics Proteomics Bioinformatics* 21: 190–202.

32. Chang W, Cheng J, Allaire J, Sievert C, Schloerke B, Xie Y, *et al.* (2012, December 1): shiny: Web Application Framework for R. p 1.10.0.

33. Yakovlev V, Lapato DM, Rana P, Ghosh P, Frye R, Roberson-Nay R (2024): Neuron enriched extracellular vesicles' MicroRNA expression profiles as a marker of early life alcohol consumption. *Transl Psychiatry* 14: 176.

34. Lewohl JM, Nunez YO, Dodd PR, Tiwari GR, Harris RA, Mayfield RD (2011): Up-Regulation of

MicroRNAs in Brain of Human Alcoholics: MICRORNAS IN HUMAN ALCOHOLICS. *Alcohol Clin Exp Res* 35: 1928–1937.

35. Ibáñez F, Ureña-Peralta JR, Costa-Alba P, Torres J-L, Laso F-J, Marcos M, *et al.* (2020): Circulating MicroRNAs in Extracellular Vesicles as Potential Biomarkers of Alcohol-Induced Neuroinflammation in Adolescence: Gender Differences [no. 18]. *Int J Mol Sci* 21: 6730.
36. Ureña-Peralta JR, Alfonso-Loeches S, Cuesta-Diaz CM, García-García F, Guerri C (2018): Deep sequencing and miRNA profiles in alcohol-induced neuroinflammation and the TLR4 response in mice cerebral cortex. *Sci Rep* 8: 15913.
37. Pers TH (2016): Gene set analysis for interpreting genetic studies. *Hum Mol Genet* 25: R133–R140.
38. Ivanova L, Rangel-Huerta OD, Tartor H, Dahle MK, Uhlig S, Fæste CK (2024): Metabolomics and Multi-Omics Determination of Potential Plasma Biomarkers in PRV-1-Infected Atlantic Salmon. *Metabolites* 14: 375.
39. Wang J, Liang J, Wang J, Shan F, Cao Y, Zhou X, *et al.* (2024): Evaluation of plasma-derived extracellular vesicles miRNAs and their connection with hippocampal mRNAs in alcohol use disorder. *Life Sci* 351: 122820.
40. Gowen AM, Odegaard KE, Hernandez J, Chand S, Koul S, Pendyala G, Yelamanchili SV (2021): Role of microRNAs in the pathophysiology of addiction. *WIREs RNA* 12: e1637.
41. Coleman LG, Crews FT (2018): Innate Immune Signaling and Alcohol Use Disorders. In: Grant KA, Lovinger DM, editors. *The Neuropharmacology of Alcohol*, vol. 248. Cham: Springer International Publishing, pp 369–396.
42. Bao C, Li Y, Huan L, Zhang Y, Zhao F, Wang Q, *et al.* (2015): NF-κB signaling relieves negative regulation by miR-194 in hepatocellular carcinoma by suppressing the transcription factor HNF-1α. *Sci Signal* 8. https://doi.org/10.1126/scisignal.aaa8441
43. Noutsios GT, Thorenoor N, Zhang X, Phelps DS, Umstead TM, Durrani F, Floros J (2017): SP-A2 contributes to miRNA-mediated sex differences in response to oxidative stress: pro-inflammatory, anti-apoptotic, and anti-oxidant pathways are involved. *Biol Sex Differ* 8: 37.
44. Rodrigues PM, Afonso MB, Simão AL, Islam T, Gaspar MM, O'Rourke CJ, *et al.* (2023): miR □21□5p promotes NASH □related hepatocarcinogenesis. *Liver Int* 43: 2256–2274.
45. Obad A, Peeran A, Little JI, Haddad GE, Tarzami ST (2018): Alcohol-Mediated Organ Damages: Heart and Brain. *Front Pharmacol* 9. https://doi.org/10.3389/fphar.2018.00081
46. Bagnardi V, Rota M, Botteri E, Tramacere I, Islami F, Fedirko V, *et al.* (2015): Alcohol consumption and site-specific cancer risk: a comprehensive dose–response meta-analysis. *Br J Cancer* 112: 580–593.
47. Maddern XJ, Ursich LT, Bailey G, Pearl A, Anversa RG, Lawrence AJ, Walker LC (2024): Sex Differences in Alcohol Use: Is It All About Hormones? *Endocrinology* 165.

https://doi.org/10.1210/endocr/bqae088

48. Flores-Bonilla A (2020): Sex Differences in the Neurobiology of Alcohol Use Disorder. *Alcohol Res Curr Rev* 40: 03.

49. Guinle MIB (2020): The Role of Stress, Trauma, and Negative Affect in the Development of Alcohol Misuse and Alcohol Use Disorders in Women. *Alcohol Res Curr Rev* 40. https://doi.org/10.35946/arcr.v40.2.05

50. Bahar ME, Kim HJ, Kim DR (2023): Targeting the RAS/RAF/MAPK pathway for cancer therapy: from mechanism to clinical studies. *Signal Transduct Target Ther* 8. https://doi.org/10.1038/s41392-023-01705-z

51. Ghafour AA, Odemis DA, Tuncer SB, Kurt B, Saral MA, Erciyas SK, *et al.* (2021): High expression level of miR-1260 family in the peripheral blood of patients with ovarian carcinoma. *J Ovarian Res* 14. https://doi.org/10.1186/s13048-021-00878-x

52. Kim DH, Park H, Choi YJ, Kang M-H, Kim T-K, Pack C-G, *et al.* (2021): Exosomal miR-1260b derived from non-small cell lung cancer promotes tumor metastasis through the inhibition of HIPK2. *Cell Death Dis* 12. https://doi.org/10.1038/s41419-021-04024-9

53. Morita T, Fujiwara T, Yoshida A, Uotani K, Kiyono M, Yokoo S, *et al.* (2020): Clinical relevance and functional significance of cell-free microRNA-1260b expression profiles in infiltrative myxofibrosarcoma. *Sci Rep* 10. https://doi.org/10.1038/s41598-020-66120-8

54. Park S, Kim J, Cho Y, Ahn S, Kim G, Hwang D, *et al.* (2022): Promotion of tumorigenesis by miR□1260b–targeting *CASP8*: Potential diagnostic and prognostic marker for breast cancer. *Cancer Sci* 113: 2097–2108.

55. Li Y, Sui S, Goel A (2024): Extracellular vesicles associated microRNAs: Their biology and clinical significance as biomarkers in gastrointestinal cancers. *Semin Cancer Biol* 99: 5–23.

56. Pla A, Pascual M, Renau-Piqueras J, Guerri C (2014): TLR4 mediates the impairment of ubiquitin-proteasome and autophagy-lysosome pathways induced by ethanol treatment in brain. *Cell Death Dis* 5: e1066–e1066.

57. Pla A, Pascual M, Guerri C (2016): Autophagy Constitutes a Protective Mechanism against Ethanol Toxicity in Mouse Astrocytes and Neurons ((T. Amédée, editor)). *PLOS ONE* 11: e0153097.

58. Yu Z, Lin S, Gong X, Zou Z, Yang X, Ruan Y, *et al.* (2024): The role of macroautophagy in substance use disorders. *Ann N Y Acad Sci*. https://doi.org/10.1111/nyas.15272

59. Ni H-M, Du K, You M, Ding W-X (2013): Critical Role of FoxO3a in Alcohol-Induced Autophagy and Hepatotoxicity. *Am J Pathol* 183: 1815–1825.

60. Huang Y, Flentke GR, Smith SM (2024): Alcohol induces p53-mediated apoptosis in neural crest by stimulating an AMPK-mediated suppression of TORC1, S6K, and ribosomal biogenesis. *Reprod Toxicol* 130: 108747.

61. Menk M, Graw JA, Poyraz D, Möbius N, Spies CD, Von Haefen C (2018): Chronic Alcohol Consumption Inhibits Autophagy and Promotes Apoptosis in the Liver. *Int J Med Sci* 15: 682–688.

62. Lista P, Straface E, Brunelleschi S, Franconi F, Malorni W (2011): On the role of autophagy in human diseases: a gender perspective. *J Cell Mol Med* 15: 1443–1457.

63. Oliván S, Calvo AC, Manzano R, Zaragoza P, Osta R (2014): Sex Differences in Constitutive Autophagy. *BioMed Res Int* 2014: 1–5.

64. Martínez De Toda I, González-Sánchez M, Díaz-Del Cerro E, Valera G, Carracedo J, Guerra-Pérez N (2023): Sex differences in markers of oxidation and inflammation. Implications for ageing. *Mech Ageing Dev* 211: 111797.

65. Mogos MF, Salemi JL, Phillips SA, Piano MR (2019): Contemporary Appraisal of Sex Differences in Prevalence, Correlates, and Outcomes of Alcoholic Cardiomyopathy. *Alcohol Alcohol* 54: 386–395.

66. Kato K, Yamamoto Y, Izawa S (2011): Severe ethanol stress induces assembly of stress granules in *Saccharomyces cerevisiae*. *Yeast* 28: 339–347.

67. Cheung SWM, Yiu JHC, Chin KTC, Cai J, Xu A, Wong CM, Woo CW (2024): Content of stress granules reveals a sex difference at the early phase of cold exposure in mice. *Am J Physiol-Endocrinol Metab* 326: E29–E37.

68. Zhang Y, Zhao Y, Tian C, Wang J, Li W, Zhong C (2018): Differential exosomal microRNA profile in the serum of a patient with depression. *Eur J Psychiatry* 32: 105–112.

69. McManus DD, Rong J, Huan T, Lacey S, Tanriverdi K, Munson PJ, *et al.* (2017): Messenger RNA and MicroRNA transcriptomic signatures of cardiometabolic risk factors. *BMC Genomics* 18. https://doi.org/10.1186/s12864-017-3533-9

70. Erol A, Karpyak VM (2015): Sex and gender-related differences in alcohol use and its consequences: Contemporary knowledge and future research considerations. *Drug Alcohol Depend* 156: 1–13.

71. Ibáñez F, Montesinos J, Area-Gomez E, Guerri C, Pascual M (2021): Ethanol Induces Extracellular Vesicle Secretion by Altering Lipid Metabolism through the Mitochondria-Associated ER Membranes and Sphingomyelinases. *Int J Mol Sci* 22: 8438.

72. Kosaka N, Iguchi H, Ochiya T (2010): Circulating microRNA in body fluid: a new potential biomarker for cancer diagnosis and prognosis. *Cancer Sci* 101: 2087–2092.

73. Mittelbrunn M, Gutiérrez-Vázquez C, Villarroya-Beltri C, González S, Sánchez-Cabo F, González MÁ, *et al.* (2011): Unidirectional transfer of microRNA-loaded exosomes from T cells to antigen-presenting cells. *Nat Commun* 2. https://doi.org/10.1038/ncomms1285

74. McCaul ME, Roach D, Hasin DS, Weisner C, Chang G, Sinha R (2019): Alcohol and Women: A Brief Overview. *Alcohol Clin Exp Res* 43: 774–779.

75. Das S, Mukhopadhyay I (2021): TiMEG: an integrative statistical method for partially missing multi-omics data. *Sci Rep* 11. https://doi.org/10.1038/s41598-021-03034-z

76. Cavill R, Jennen D, Kleinjans J, Briedé JJ (2016): Transcriptomic and metabolomic data integration. *Brief Bioinform* 17: 891–901.

77. Schwarzenbach H, Da Silva AM, Calin G, Pantel K (2015): Data Normalization Strategies for MicroRNA Quantification. *Clin Chem* 61: 1333–1342.